Widely tunable chaotic fiber laser for WDM-PON detection*

ZHANG Juan (张娟)[1], **YANG Ling-zhen** (杨玲珍)[1,2]**, **XU Nai-jun** (徐乃军)[1], **WANG Juan-fen** (王娟芬)[1], **ZHANG Zhao-xia** (张朝霞)[1], **and LIU Xiang-lian** (刘香莲)[1]

1. *Institute of Optoelectronic Engineering, College of Physics and Optoelectronics, Taiyuan University of Technology, Taiyuan 030024, China*
2. *Key Lab of Advanced Transducers and Intelligent Control System, Ministry of Education, Taiyuan University of Technology, Taiyuan 030024, China*

(Received 7 February 2014)

A widely tunable high precision chaotic fiber laser is proposed and experimentally demonstrated. A tunable fiber Bragg grating (TFBG) filter is used as a tuning element to determine the turning range from 1533 nm to 1558 nm with a linewidth of 0.5 nm at any wavelength. The wide tuning range is capable of supporting 32 wavelength-division multiplexing (WDM) channels with 100 GHz channel spacing. All single wavelengths are found to be chaotic with 10 GHz bandwidth. The full width at half maximum (FWHM) of the chaotic correlation curve of the different wavelengths is on a picosecond time scale, thereby offering millimeter spatial resolution in WDM detection.

Document code: A **Article ID:** 1673-1905(2014)03-0232-5

DOI 10.1007/s11801-014-4014-x

Wavelength tunable fiber lasers are extensively investigated because of the large demands in wavelength division multiplexing (WDM) networks, optical detection, and fiber sensor systems[1–3]. A tunable fiber laser is usually built with various tunable components, such as tunable band pass filter, fiber Fabry–Perot tunable filter, and fiber Bragg grating filter[4–6]. Many methods and techniques have been studied and reported. Wei Yang[7] achieved continuous wavelength tuning using a single stage polarization-independent acousto-optic tunable filter in an erbium-doped fiber ring laser. In 2013, a wavelength tunable erbium-doped fiber ring laser based on a silicon micro-ring resonator was proposed and a 35.2 nm bandwidth with a tuning step of 2 nm was achieved[8]. In the same year, Pei Yang[9] experimentally generated over 40 single-mode wavelengths with 100 GHz spacing using a self-seeding reflective semiconductor optical amplifier. Among the numerous tuning methods, the tuning fiber laser based on fiber Bragg grating can effectively reduce the insertion loss.

Chaotic lasers are extensively studied in high-speed chaotic secure communication, anti-interference ranging, and sensing field because of their natural confidentiality, anti-interference, and non-predictability[10–12]. Fiber lasers can generate chaotic bandwidth of at least tens of gigahertz[13]. The wide bandwidth leads to high-speed data transmission and high precision measurement resolution in the WDM network communication and detection. Moreover, the measurement resolution of the chaotic optical signal is not related with fiber length[14]. Therefore, the tunable chaotic laser is a promising light source in the future application of the WDM network. This paper experimentally demonstrates a continuously tunable chaotic fiber laser based on an ultra-long erbium-doped fiber ring laser (ULEDFRL) using a tunable fiber Bragg grating (TFBG) filter as the tuning component. We analyze the characteristics of the tunable chaotic laser in each wavelength and carry out corresponding experiment to detect 8 WDM wavelengths to further prove the excellent properties of the tunable chaotic laser.

Fig.1 shows the experimental setup for the proposed tunable chaotic fiber laser. Fig.1(a) shows that the 980 nm semiconductor laser is used to pump an 8 m long erbium-doped fiber by a 980/1550 nm WDM. The polarization isolator forces the light to operate unidirectionally. The polarization controller (PC) is applied to ensure that the fiber laser can work in a proper polarization state. The 10 km ultra-long single-mode fiber in the cavity supports the strong nonlinear effect. The fine-tuning of the wavelength is achieved by the TFBG filter, and the tunable range is from 1530 nm to 1560 nm. The 90:10 output coupler1 gives 10% of the lasing light for the output detection. The characteristics of the chaotic output are analyzed using an oscilloscope (OSC) and a spectrum analyzer (OSA) together with a 12 GHz photodetector (PD).

* This work has been supported by the National Natural Science Foundation of China (No.61107033), the Program for the Top Young Academic Leaders of Higher Learning Institutions of Shanxi, and the Open Research Fund of State Key Laboratory of Transient Optics and Photonics, Chinese Academy of Sciences (No.SKLST201103).

** E-mail: office-science@tyut.edu.cn

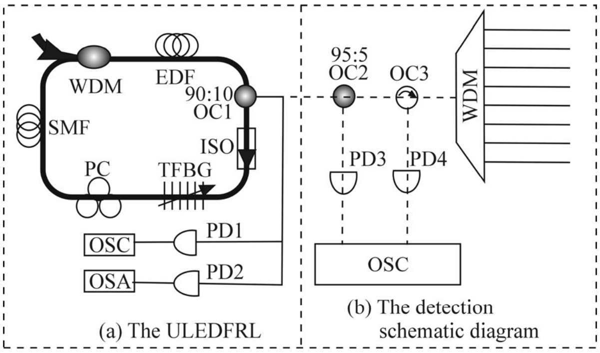

Fig.1 Experimental setup of the proposed tunable chaotic fiber laser

The experiment is carried out without the TFBG in the ULEDFRL. We adjust the PC and observe the output dynamics of the ULEDFRL under a fixed power pump. When the PC is placed in a proper position, a wideband frequency spectrum could be obtained in the spectrum analyzer. Then, we maintain the PC at a fixed position and continuously increase the pump current. When the pump current is increased to 180 mA, the chaotic states are observed at the OSC and OSA and fixed well to 450 mA. Fig.2 demonstrates the chaotic states for the pump current of 280 mA. The noise-like time sequence in Fig.2(a) shows random intensity fluctuations. The wideband power spectrum in Fig.2(b) is flat and smooth. The auto-correlation curve, which is delta function like in Fig.2(c), is sharp and thin, the full width at half maximum (FWHM) is about 75 ps, and the central wavelength of the optical spectrum in Fig.2(d) is 1564 nm. Then, we add the TFBG in the cavity and tune it carefully. The tuning filter is accurate, highly efficient, and continuous. The fiber laser is continuously tuned from 1533 nm to 1558 nm. Fig.3 shows the 32 international telecommunication union (ITU) channels with 100 GHz channel spacing for a pump current of 280 mA. The start and stop wavelengths are 1533.47 nm and 1558.17 nm, respectively. Chaotic oscillation with a pump current above the threshold is observed at any wavelength presented.

The wavelengths of 1551.72 nm, 1552.52 nm, 1553.33 nm, 1554.13 nm, 1554.94 nm, 1555.75 nm, 1556.55 nm and 1557.36 nm are selected as representative samples to demonstrate the characteristics of the tunable chaotic fiber laser.

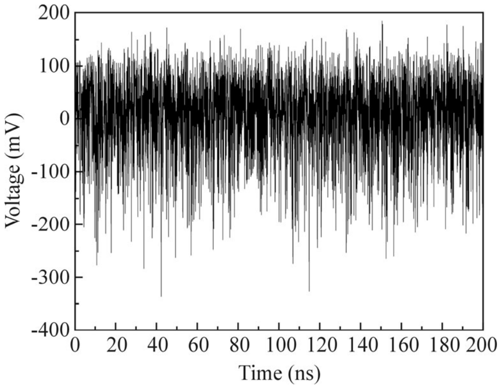

(a) Noise-like time sequence

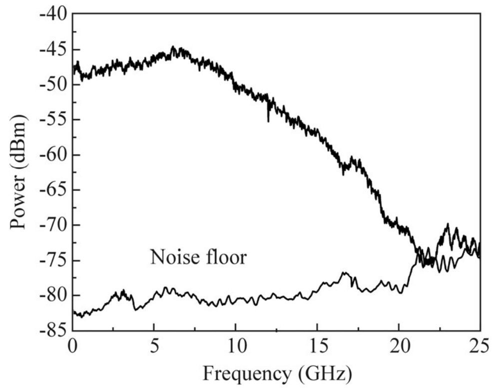

(b) Wideband power spectrum

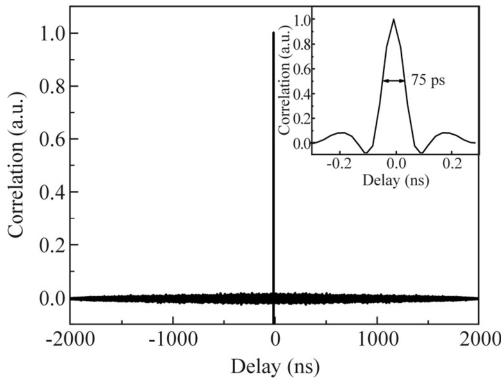

(c) Auto-correlation curve

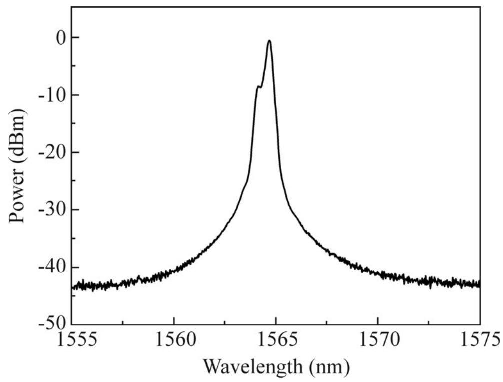

(d) Optical spectrum

Fig.2 Chaotic output of ULEDFRL without TFBG at 280 mA

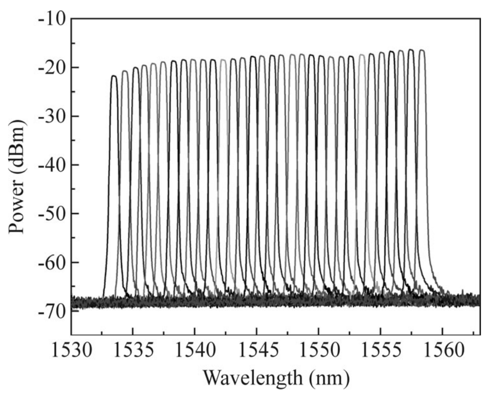

Fig.3 Optical spectrum of the wavelength tunable ULEDFRL with TFBG

Fig.4 shows the outputs of the fiber laser with 1554.13 nm, 1555.75 nm, 1556.55 nm and 1557.36 nm from the top to the bottom. The rapid random intensity fluctuations of the time sequence in Fig.4(a) column, the delta-function-like correlation characteristics in Fig.4(b) column, and the broad band spectra in Fig.4(c) column all indicate that the tunable fiber laser works in chaotic states. The FWHMs of the auto-correlation curves in the studied wavelengths in Fig.4(b) column are about 73 ps. Fig.4(c) column shows the power spectra with different pump current values. The –3 dB bandwidth, which is about 10 GHz, is enhanced with the increase of the pump current because higher pump current stimulates stronger nonlinear effect that leads to a broader band spectrum. The chaotic laser at other wavelengths exhibits similar characteristics.

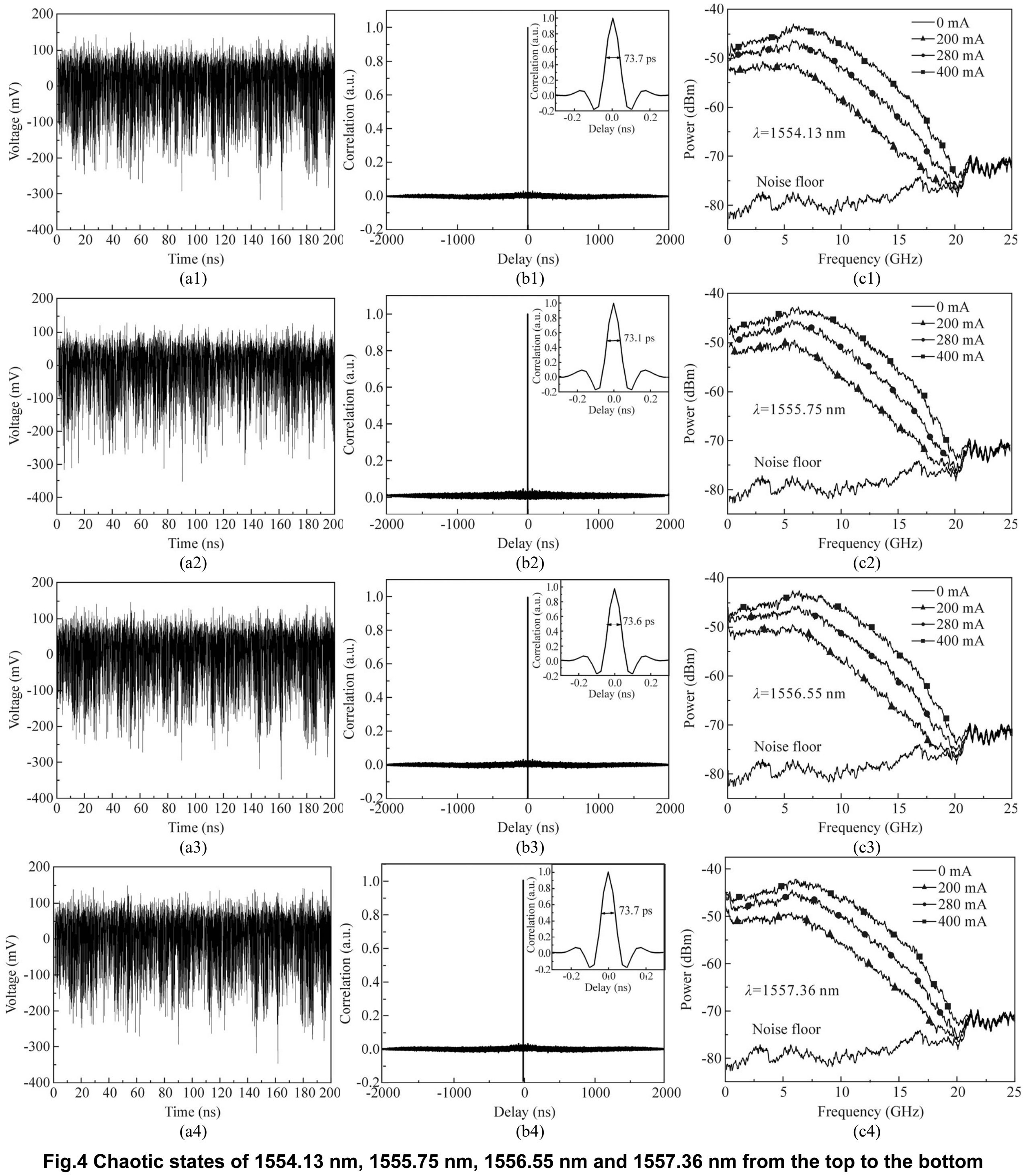

Fig.4 Chaotic states of 1554.13 nm, 1555.75 nm, 1556.55 nm and 1557.36 nm from the top to the bottom

The broad bandwidth and thin auto-correlation curve of the tunable chaotic fiber laser demonstrate a high measurement precision. We estimate the spatial resolution by the FWHM of the chaotic auto-correlation curve. Fig.5 shows the FWHMs of different wavelengths. Compared with the chaotic states before splitting (Fig.2), the FWHM is almost the same at 280 mA (arrow pointed in Fig.5). This result demonstrates that the bandwidth of the tunable chaotic laser is broader than that of the PD, so the difference could not be observed within the filter. The FWHM decreases with the increase of the pump current in all wavelengths, but no noticeable regularity is observed in different wavelengths when the pump current is fixed. The reason is that the larger pump current stimulates stronger nonlinear effect which increases the chaotic bandwidth, resulting in the decrease of the FWHM with the increase of pump current. However, the chaotic laser exhibits unique temporal and spectral characteristics, and slight fluctuations are not forecasted. The FWHM varies from 60 ps to 90 ps, and the pump current varies from 200 mA to 400 mA in all observed wavelength ranges. According to $c\bullet\tau/2n$, where c is the speed of light in vacuum, τ is the time delay corresponding to the FWHM, and n is the refraction index of the fiber, the spatial resolution is 6 mm to 9 mm. This resolution indicates that the wavelength tunable chaotic fiber laser could achieve a millimeter measurement resolution.

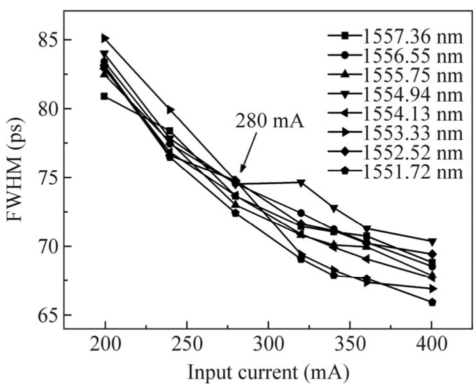

Fig.5 Relationship between FWHM and pump current in different wavelengths

Fig.6 shows the *P–I* curves of the wavelength tunable ULEDFRL. The output power linearly increases with the pump current in each wavelength. The slope efficiency and threshold change with the wavelength because of the TFBG property. The wavelength tunable ULEDFRL works in chaotic states when the pump current is from 180 mA to 450 mA. The wide chaotic field provides great convenience for the applications.

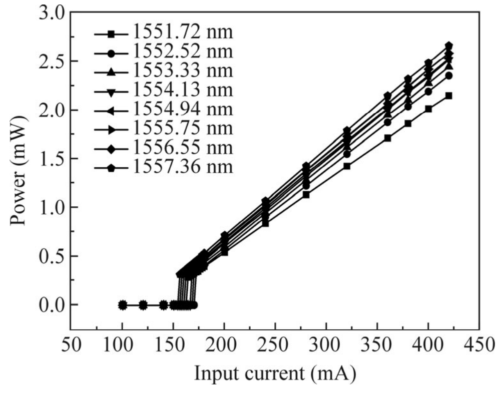

Fig.6 *P–I* curves of the wavelength tunable ULEDFRL

To demonstrate the feasibility of the tunable chaotic fiber laser, we experimentally carry out the WDM-PON detection with the 8 WDM wavelengths. The detection schematic diagram is shown in Fig.1(b). The output chaotic laser from the ULEDFRL is split into two parts by output coupler2: 5% is used as the reference signal, and the other 95% serves as the detectable signal. The detectable signal is launched into the WDM-PON channels and reflected at the fault position through the optical circulator3. The reference signal and the reflected signal of the detection light are detected by PD3 and PD4 with 1 GHz bandwidth. The fault position is located by correlation of the two signals. The different channels are detected by sweeping the chaotic laser. The detection results with a low signal to noise ratio are shown in Fig.7(a). The detection distances of the 8 wavelengths are 1235.82 m, 1186.86 m, 1138.10 m, 1091.07 m, 863.40 m, 816.37 m, 767.40 m and 718.64 m. The small drop of the correlation peaks with different wavelengths is attributed to the characteristic loss of the detection fiber. Fig.7(b) shows the minimum distance that could be detected in the experiment, which corresponds to the 4 cm spatial resolution and is the same in all studied wavelengths. The spatial resolution in the detection is limited by the 1 GHz PD. The measurement examples show that the wavelength tunable laser could accurately detect the WDM-PON at any single wavelength, and if the bandwidths of the PD are all 12 GHz, the millimeter spatial resolution can be obtained.

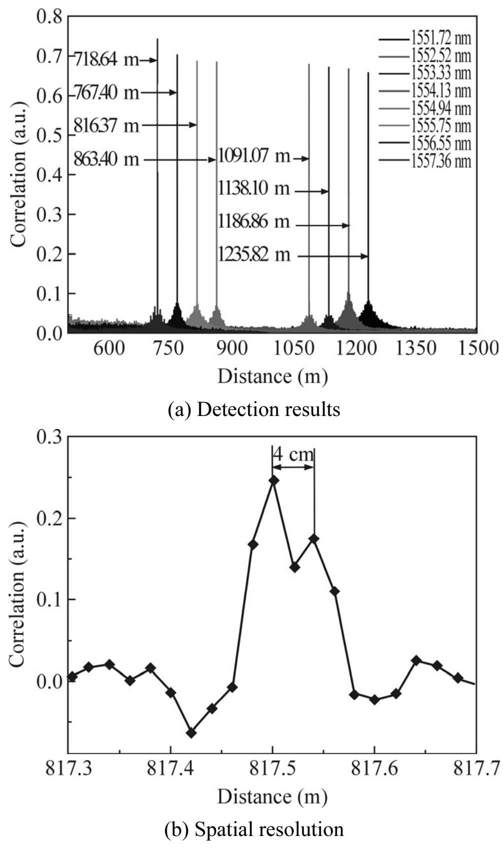

Fig.7 Detection results of 8 channels of the WDM-PON using the wavelength tunable chaotic laser

We experimentally demonstrate a widely tunable high precision chaotic fiber laser. The chaotic fiber laser is constructed by a ULEDFRL and a TFBG. The 25 nm wide tunable wavelength range is obtained and the 32 WDM channels with 100 GHz channel spacing are supported. Each of the 32 ITU channels works in chaotic states with a bandwidth of about 10 GHz. The auto-correlation curve of the wideband time sequence generated in the fiber chaotic laser has a peak with a picosecond time scale, offering a millimeter spatial resolution for the correlation-based WDM-PON detection. The WDM detection experiment verifies the reasonable application of the tunable chaotic fiber laser.

References

[1] Y. W. Song, S. A. Havstad, D. Starodubov, Y. Xie, A. E. Willner and J. Feinberg, IEEE Photonics Technology Letters **13**, 1167 (2001).

[2] W. Shin, B. A. Yu, Y. L. Lee, Y. C. Noh, D. K. Ko and K. Oh, Optics Communications **282**, 1191 (2009).

[3] Y. J. Rao, Z. L. Ran and R. R. Chen, Optics Letters **31**, 2684 (2006).

[4] H. X. Chen, F. Babin, M. Leblanc and G. W. Schinn, IEEE Photonics Technology Letters **15**, 185 (2003).

[5] Y. L. Ju, Y. Xu and F. F. Zhong, Laser Physics and Laser Technologies and 2010 Academic Symposium on Optoelectronics Technology, 10th Russian-Chinese Symposium on IEEE, 112 (2010).

[6] S. J. Feng, Q. H. Mao, Y. Y. Tian, Y. Ma, W. C. Li and L. Wei, IEEE Photonics Technology Letters **25**, 323 (2013).

[7] W. Yang, Y. Liu, L. F. Xiao and Z. X. Yang, Journal of Lightwave Technology **28**, 118 (2010).

[8] L. G. Yang, C. H. Yeh, C. Y. Wong, C. W. Chow, F. G. Tseng and H. K. Tsang, Optics Express **21**, 2869 (2013).

[9] P. Yang, S. L. Xiao, H. L. Feng, M. H. Bi, J. Shi and Z. Zhou, Chinese Optics Letters **11**, 040602 (2013).

[10] Z. G. Li, K. Li, C. Y. Wen and Y. C. Soh, Transctions on Communications **51**, 1306 (2003).

[11] F. Y. Lin and J. M. Liu, Journal of Quantum Electronics **40**, 815 (2004).

[12] L. Yu, J. P. Barbot, G. Zheng and H. Sun, IEEE Signal Processing Letters **17**, 731 (2010).

[13] L. Z. Yang, L. Zhang, R. Yang, L. Yang, B. H. Yue and P. Yang, Optics Communications **285**, 143 (2012).

[14] Z. H. Xie, L. Xia, Y. W. Wang, C. L. Yang, C. Cheng and D. M. Liu, IEEE Photonics Technology Letters **25**, 709 (2013).